Information Sciences 214 (2012) 20–34

Contents lists available at SciVerse ScienceDirect

Information Sciences

journal homepage: www.elsevier.com/locate/ins

Comprehensive QoS analysis of enhanced distributed channel access in wireless local area networks

Jia Hu [a], Geyong Min [b,*], Weijia Jia [c], Mike E. Woodward [b]

[a] Department of Computer Science, Liverpool Hope University, Liverpool L16 9JD, UK
[b] Department of Computing, School of Informatics, University of Bradford, Bradford BD7 1DP, UK
[c] Department of Computer Science, City University of Hong Kong, 83 Tat Chee Ave., Hong Kong

ARTICLE INFO

Article history:
Received 23 October 2011
Received in revised form 3 May 2012
Accepted 16 May 2012
Available online 24 May 2012

Keywords:
Medium access control
QoS
Wireless LAN
Transmission opportunity
Queueing analysis

ABSTRACT

Wireless information networks satisfy the users' desirable requirements for mobility and relocation and thus have experienced tremendous growth in recent years. The Enhanced Distributed Channel Access (EDCA) is a promising Medium Access Control (MAC) protocol for provisioning of Quality-of-Service (QoS) in Wireless Local Area Networks (WLANs). This protocol specifies three important QoS schemes including Arbitrary Inter-Frame Space (AIFS), Contention Window (CW) and Transmission Opportunity (TXOP). Analytical models of EDCA reported in the literature have been primarily developed for the AIFS, CW, and TXOP schemes, separately. This paper proposes a comprehensive analytical model to accommodate the *integration* of these three QoS schemes in WLANs with finite buffer capacity under unsaturated traffic loads. The important QoS performance metrics in terms of throughput, delay, delay jitter, and frame loss probability are derived. The accuracy of the model is validated through extensive simulation experiments. Performance results reveal that the TXOP can support QoS differentiation, improve the system performance significantly and outperform AIFS and CW owing to its unique burst transmission property. Furthermore, the results demonstrate that the buffer size has considerable impact on the QoS of EDCA, highlighting the importance of taking the buffer size into account for design and analysis of MAC protocols.

1. Introduction

Information systems have revolutionized the world significantly and become pervasive in our daily life. As business, research, and entertainment shift towards more mobile, and people require constant access to information anytime and anywhere, the need for mobile and wireless networks keeps increasing. By freeing the user from the cord, wireless information networks [14,19,32] such as Wireless Local Area Networks (WLANs), cellular systems, and sensor networks satisfy the users' desirable requirements for mobility and relocation and thus have experienced tremendous growth in recent years.

The IEEE 802.11 WLANs have experienced impressive success owing to their attractive properties, such as low cost and easy deployment. The fundamental Medium Access Control (MAC) protocol of the IEEE 802.11 standard is Distributed Coordination Function (DCF) [16], which is based on the Carrier Sense Multiple Access with Collision Avoidance (CSMA/CA) and Binary Exponential Backoff (BEB) mechanism. As the DCF was originally designed for handling the best-effort traffic only, it is unable to support differentiated Quality-of-Service (QoS). However, with the rapid growth of wireless multimedia applications, there is an ever-increasing demand for provisioning of QoS differentiation in WLANs.

* Corresponding author.
E-mail addresses: huj@hope.ac.uk (J. Hu), g.min@brad.ac.uk (G. Min), wei.jia@cityu.edu.hk (W. Jia), m.e.woodward@brad.ac.uk (M.E. Woodward).

0020-0255/$ - see front matter © 2012 Elsevier Inc. All rights reserved.
http://dx.doi.org/10.1016/j.ins.2012.05.013

To support the MAC-level QoS, an enhanced version of the IEEE 802.11 protocol [16], namely IEEE 802.11e, has been proposed. This protocol employs a channel access function called Hybrid Coordination Function (HCF) [16], which comprises the contention-based Enhanced Distributed Channel Access (EDCA) and centrally controlled Hybrid Coordinated Channel Access (HCCA). The EDCA is the fundamental and mandatory mechanism of 802.11e, whereas HCCA is optional and requires complex scheduling algorithms for resource allocation. The EDCA classifies the traffic flows into four Access Categories (ACs) [16], each of which is associated to a separate transmission queue and behaves independently. These ACs are differentiated through adjusting the parameters of Arbitrary Inter-frame Space (AIFS), Contention Window (CW) and Transmission Opportunity (TXOP) limit [16]. The AIFS and CW decide the deferring time and the backoff time of the AC that contends for the channel, respectively, while the TXOP limit controls the channel occupation time of the AC that gains the channel.

Significant research efforts have been devoted to developing the analytical performance model for the QoS differentiation schemes specified in the EDCA protocol [1,2,6–8,10–13,15,17,18,20,21,23,25,27–31,33–38,40–42]. The majority of these existing models were developed under the assumption of saturated working conditions where all the ACs have frames for transmission anytime [12,13,15,21,23,29–31,33,35,37,40–42]. Since the traffic loads in the practical network environments are mainly unsaturated [5,9,22,24], it is imperative to develop analytical models for EDCA in the presence of unsaturated traffic conditions. However, the existing analytical models reported in the current literature have been primarily focused on the AIFS, CW, and TXOP schemes, *separately* [1,6–8,10,20,25–28,34,36]. In addition, these models are based on the assumptions that the MAC buffer has either a very small size [20,34] or an infinite capacity [1,6,7,25,36]. These assumptions cannot capture the realistic working conditions of practical WLANs. With the aim of conducting a thorough and deep investigation of the QoS performance of EDCA, this paper proposes a comprehensive analytical model to accommodate the combination of all three QoS schemes of EDCA under unsaturated traffic loads. The major contributions of this paper include:

(1) A new three-dimensional (3D) Markov chain is proposed to analyze the backoff procedure of EDCA. To address the difficulties of analyzing the TXOP burst transmission, the queue at each AC is modelled as a bulk service queueing system with finite capacity.
(2) The proposed analytical model can handle the large MAC buffer size without heavily increasing the complexity of the solution. Moreover, this model considers the virtual collisions between ACs in a station and takes into account the effects of the frame retry limit in order to capture the behavior of EDCA accurately.
(3) This comprehensive analytical model incorporates the combination of the QoS differentiation schemes in terms of AIFS, CW, and TXOP simultaneously. The performance metrics including throughput, end-to-end delay, delay jitter, and frame loss probability are derived. The accuracy of the model is validated by comparing the analytical results to those obtained from extensive NS-2 simulation experiments.
(4) The analytical results show that the TXOP scheme can support service differentiation and also improve the network performance, whereas the AIFS and CW schemes can provide QoS differentiation only. Moreover, the analysis demonstrates that the MAC buffer size has considerable impact on the QoS performance of ACs in IEEE 802.11e WLANs. The performance results highlight the importance of using the combination of these three schemes in WLANs and demonstrate the value of this comprehensive analytical model as a cost-efficient tool for performance evaluation of EDCA.

The remainder of this paper is organized as follows. Section 2 briefly introduces the EDCA protocol. Section 3 reviews the related work in the literature and presents the originality of this study. Section 4 elaborates on the derivation of the analytical model. After validating the accuracy of the model and conducting performance analysis in Section 5, we conclude this paper in Section 6.

2. Enhanced Distributed Channel Access (EDCA)

EDCA was designed to improve the performance of DCF and provide the differentiated QoS [16]. Traffic of different classes is assigned to one of four ACs, which is associated to a separate transmission queue and behaves independently. The QoS of these ACs is differentiated through assigning various EDCA parameters including AIFS values, CW sizes, and TXOP limits. Specifically, a smaller AIFS/CW leads to a larger probability of winning the contention for the channel. On the other hand, the larger the TXOP limit, the longer the channel holding time of the AC winning the contention.

In the EDCA protocol, the channel is sensed before an AC attempts to transmit frames. If the channel is detected idle for an AIFS, the transmission starts. Otherwise, the AC defers until the channel is detected idle for an AIFS, and then generates a random backoff counter. The AIFS for a given AC is defined as $AIFS_{[AC]} = SIFS + AIFSN_{[AC]} \times aSlotTime$, where $AIFSN_{[AC]}$ ($AIFSN_{[AC]} \geqslant 2$) represents the number of time slots in $AIFS_{[AC]}$ and *aSlotTime* denotes the duration of a time slot [16].

The value of the backoff counter is uniformly chosen between zero and $CW_{[AC]}$, which is initially set to $CW_{\min[AC]}$ and doubled after each unsuccessful transmission until it reaches the maximum value $CW_{\max[AC]}$. It is reset to $CW_{\min[AC]}$ after the transmission succeeds or the number of retransmission attempts reaches a retry limit. The backoff counter is decreased by one for each time slot [16] when the channel is idle, halted when the channel becomes busy and resumed when the channel is idle again for an AIFS. An AC transmits when its backoff counter becomes zero. When the backoff counters of different

ACs within a station decrease to zero simultaneously, the frame from the highest priority AC among the contending ones is selected for transmission on the channel, while the others suffer from a *virtual collision* and invoke the backoff procedure.

Upon winning the access to the channel, the AC transmits the frames available in its buffer consecutively provided that the duration of transmission does not exceed the specific TXOP limit [16]. Each frame is acknowledged by an Acknowledgement (ACK) after a Short Inter-frame Space (SIFS) interval. The next frame is transmitted immediately after receiving the ACK and waiting for an SIFS. If the transmission of any frame fails the burst is terminated and the AC contends again for the channel to retransmit the failed frame.

3. Literature review and originality of this work

This section first presents a detailed literature review of related work and then outlines the originality of this study.

3.1. Related work

Modelling and performance analysis of the AIFS and CW schemes specified in EDCA have received considerable research interests [1,6–8,11–13,15,17,20,21,25,27,29–31,33–35,38,40–42]. Most of these studies were based on Bianchi's two-dimensional (2D) Markov chain [3] under the assumption of saturated traffic conditions. For instance, Xiao [40] extended the Markov chain proposed in [3] to model the CW differentiation scheme of EDCA. Kong et al. [21] analyzed the AIFS and CW schemes using a 3D Markov chain where the third dimension indicates the remaining time before activating the backoff counter. Huang and Liao [12] analyzed the performance of saturation throughput and access delay of EDCA. Hwang et al. [15] presented an analytical model for EDCA with consideration of virtual collision, but the model was limited to the case that the difference between the minimum and maximum AIFS is one time slot only. Tursunova and Kim [38] proposed an EDCA mathematical model for QoS-aware differentiated multimedia mobile cloud services.

As an important QoS scheme specified in EDCA, the TXOP scheme has also attracted many research efforts, which were mainly focused on the analysis of the saturation performance [23,37,41]. Specifically, Tinnirello and Choi [37] compared the saturation throughput of the TXOP scheme coupled by different ACK policies. Li et al. [23] evaluated the saturation throughput of the TXOP scheme with the block ACK policy under noisy channel conditions. Xu et al. [41] analyzed the MAC access delay of EDCA with the AIFS, CW, and TXOP schemes under saturated conditions.

The existing models for EDCA have been primarily derived based on the assumption of saturated traffic conditions where all the stations are backlogged all the time [12,13,15,21,23,30,31,33,35,37,40–42]. Since the traffic loads in the practical network environments are mainly unsaturated [24], the development of analytical models for EDCA under unsaturated traffic conditions has also drawn much research attention [1,6–8,10,17,20,25–28,34,36]. For example, Tantra et al. [34] introduced a Markov model to derive the throughput and delay of the CW scheme in EDCA, assuming that each AC has a MAC buffer with the capacity of only one frame. Liu and Niu [25] employed an M/M/1 queueing model to analyze the EDCA with the AIFS and CW schemes. They assumed an infinite capacity of the MAC buffer. As for the TXOP scheme, Hu et al. [10] analyzed and compared the performance of the TXOP scheme coupled by different ACK policies under unsaturated traffic loads. Nguyen et al. [28] proposed a tractable model of IEEE 802.11e carrying traffic from a mixture of saturated and unsaturated (Poisson) sources, with different CW and TXOP parameters.

The performance of the AIFS, CW and TXOP schemes specified in EDCA has been primarily studied *separately* under unsaturated traffic conditions [1,6–8,10,20,25–28,34,36]. However, to the best of our knowledge, there has been only one attempt [17] to analytically modelling the combination of these three QoS schemes in EDCA under unsaturated traffic conditions. Inan et al. [17] leveraged a 3D Markov chain to capture the functionality of these three QoS schemes of EDCA, where the third dimension of the Markov chain denotes the number of backlogged frames in the transmission queue of an AC. As a result, the complexity of the solution becomes very high as the size of the transmission queue augments. Moreover, their model assumed a constant probability of packet arrival per state, which is unable to capture the stochastic properties of packet arrivals.

3.2. Originality of this work

The comprehensive analytical model presented in this paper is distinguishing from those reported in the current literature in various aspects. This model is able to incorporate the three QoS schemes of EDCA (i.e., AIFS, CW and TXOP) simultaneously in WLANs with finite buffer capacity in the presence of unsaturated traffic loads. Unlike the model reported in [17], we employ an approach combining the Markov chain and queueing theory to analyze the backoff procedure and the burst transmission procedure of EDCA. As a result, the proposed analytical model holds the following advantages: (1) it can handle a large number of MAC buffer size without heavily increasing the complexity of the solution; (2) it can derive the delay jitter that is an important performance measure for delay-sensitive applications.

Moreover, the new 3D Markov chain proposed in this paper to analyze the backoff procedure of EDCA is more general and can capture the behavior of EDCA more accurately than existing EDCA models based on a 3D Markov chain where the third dimension denotes the number of remaining time slots to complete the AIFS period [15,21,33]. Because this proposed 3D Markov chain takes into account the AIFS differentiation, virtual collision, frame retry limit, and details of the backoff rule, which were not properly or comprehensively captured in existing models. For instance, the models reported in [33] were limited to the case where the difference between the minimum AIFS ($AIFS_{\min}$) and maximum AIFS ($AIFS_{\max}$) is one time slot only. In [21], the channel busy probability is not differentiated between the countdown and deferring periods of the backoff counter. Moreover, this model assumed that the backoff counter of an AC is immediately activated after the ACK timeout interval when the AC encounters a collision. However, in the IEEE 802.11e standard [16], the backoff counter is invoked if the channel is detected to be idle for the AIFS period after the ACK timeout interval. To capture this behavior, the 3D Markov chain proposed in this paper transits to the deferring state when the backoff stage increases due to an unsuccessful transmission.

4. Analytical model

In this section, we elaborate on the proposed analytical model for EDCA which can be used to evaluate the QoS performance metrics including throughput, end-to-end delay, delay jitter, and frame loss probability. The ACs from the lowest to highest priority are denoted by subscripts 0, 1, 2, ..., N. The transmission queue at each AC is modelled as a bulk service queueing system where the arrival traffic follows a Poisson process with rate λ_v (frames/s, $v = 0, 1, 2, \ldots, N$). The service rate of the queueing system, μ_v, is derived by analyzing the backoff and burst transmission procedures of the AC_v. With λ_v and μ_v, we can solve the bulk-service queueing system to obtain the QoS performance measures of ACs in the IEEE 802.11e WLANs.

4.1. Modelling of the backoff procedure

This subsection presents a new 3D discrete-time Markov chain to analyze the backoff procedure of EDCA. In this Markov chain, a time slot is referred to as the variable time interval between the starts of two consecutive decrements of the backoff counter. To avoid any ambiguity, in what follows, the fixed time interval (unit time) specified in the IEEE 802.11e standard [16] is called the *physical time slot*. Let $s(t)$ and $b(t)$ denote the stochastic processes representing the backoff stage and the backoff counter for a given AC, respectively. The third dimension, $c(t)$, represents the number of the remaining time slots required to complete the AIFS period of the AC ($AIFS_v$) after $AIFS_{\min}$. The 3D process $\{s(t), b(t), c(t)\}$ can be modelled as a discrete-time Markov chain as shown in Fig. 1a, with a dashed line box shown in detail in the sub-Markov chain of Fig. 1b.

The state transition probabilities of the 3D Markov chain are described as follows:

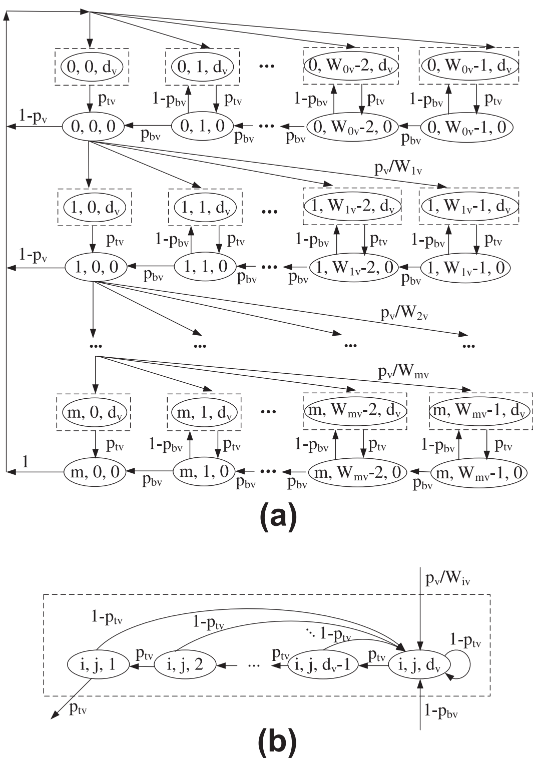

Fig. 1. The 3D Markov chain for modelling the backoff procedure of the AC_v.

$$\begin{cases} P\{i,j,0|i,j+1,0\} = p_{bv}, & 0 \leqslant i \leqslant m, \quad 0 \leqslant j \leqslant W_{iv}-2 & \text{(1a)} \\ P\{i,j,d_v|i,j,0\} = 1-p_{bv}, & 0 \leqslant i \leqslant m, \quad 1 \leqslant j \leqslant W_{iv}-1 & \text{(1b)} \\ P\{i,j,0|i,j,1\} = p_{tv}, & 0 \leqslant i \leqslant m, \quad 0 \leqslant j \leqslant W_{iv}-1 & \text{(1c)} \\ P\{i,j,k|i,j,k+1\} = p_{tv}, & 1 \leqslant k \leqslant d_v - 1 & \text{(1d)} \\ P\{i,j,d_v|i,j,k\} = 1-p_{tv}, & 1 \leqslant k \leqslant d_v & \text{(1e)} \\ P\{i,j,d_v|i-1,0,0\} = p_v/W_{iv}, & 1 \leqslant i \leqslant m, \quad 0 \leqslant j \leqslant W_{iv}-1 & \text{(1f)} \\ P\{0,j,d_v|i,0,0\} = (1-p_v)/W_{0v}, & 0 \leqslant i \leqslant m-1, \quad 0 \leqslant j \leqslant W_{iv}-1 & \text{(1g)} \\ P\{0,j,d_v|m,0,0\} = 1/W_{0v}, & 0 \leqslant j \leqslant W_{iv}-1 & \text{(1h)} \end{cases} \tag{1}$$

where p_v denotes the collision probability of the Head-of-Burst (HoB) frame transmitted from the AC_v (note that only the HoB frame needs to contend for the channel), p_{bv} is the probability that the channel is idle in a time slot after the AIFS period of the AC_v, and p_{tv} is the probability that the channel is idle in a time slot during the AIFS period of the AC_v after $AIFS_{\min}$. d_v represents the difference in the number of physical time slots between $AIFS_{\min}$ and $AIFS_v$, i.e., $d_v = AIFSN_v - AIFSN_{\min}$. m denotes the retry limit (i.e., the maximum backoff stage) and $W_{iv}(0 \leqslant i \leqslant m)$ accounts for the CW after i unsuccessful transmissions. W_{iv} is given by

$$W_{iv} = \begin{cases} 2^i W_{0v} & 0 \leqslant i \leqslant m' \\ 2^{m'} W_{0v} & m' < i \leqslant m \end{cases} \tag{2}$$

where W_{0v} and $2^{m'}W_{0v}$ represent the $CW_{\min}$ and $CW_{\max}$ of the AC_v, respectively.

The equations of the state transition probabilities account, respectively, for: Eq. (1a) The backoff counter is decreased by one after an idle time slot; (1b) The backoff counter is frozen if sensing a busy channel; (1c) The backoff counter is activated after the AIFS period; (1d) The remaining number of time slots in the AIFS period is decreased by one if the channel is detected idle in a time slot; (1e) The AC has to go through the AIFS period again if the channel is sensed busy during the AIFS period; (1f) The backoff stage increases after an unsuccessful transmission and the AC defers for the AIFS period before activating the backoff counter; (1g) After a successful transmission, the CW is reset to $CW_{\min}$; (1h) The CW is reset to $CW_{\min}$ if the retransmission attempts reach the retry limit.

Let $b_{i,j,k}$ be the stationary distribution of the 3D Markov chain with state $\{i,j,k\}$ where $i \in [0,m]$, $j \in [0, W_{iv}-1]$, and $k \in [0, d_v]$. $b_{i,j,k}$ satisfies the following normalization condition

$$1 = \sum_{i=0}^{m} \sum_{j=0}^{W_{iv}-1} b_{i,j,0} + \sum_{i=0}^{m} \sum_{j=0}^{W_{iv}-1} \sum_{k=1}^{d_v} b_{i,j,k} \tag{3}$$

Solving the 3D Markov chain, the initial state, $b_{0,0,0}$, is given by

$$b_{0,0,0} = \left[\frac{\left(1-p_{tv}^{d_v}\right)}{(1-p_{tv})p_{tv}^{d_v}} \left((1-p_{bv}) \sum_{i=0}^{m} \frac{W_{iv}-1}{2} p_v^i + \frac{1-p_v^{m+1}}{1-p_v} \right) + \sum_{i=0}^{m} \frac{W_{iv}-1}{2} p_v^i + \frac{1-p_v^{m+1}}{1-p_v} \right]^{-1} \tag{4}$$

Note that for the ACs with the minimum AIFS period, d_v equals zero. Therefore, Eq. (4) can be reduced to

$$b_{0,0,0} = \left[\sum_{i=0}^{m} \frac{W_{iv}-1}{2} p_v^i + \frac{1-p_v^{m+1}}{1-p_v} \right]^{-1} \tag{5}$$

The probability that an AC_v transmits in a randomly chosen time slot, τ'_v, when its transmission queue is non-empty, is calculated as

$$\tau'_v = \sum_{i=0}^{m} b_{i,0,0} = b_{0,0,0} \sum_{i=0}^{m} p_v^i = \frac{b_{0,0,0}(1-p_v^{m+1})}{(1-p_v)} \tag{6}$$

Note that an AC can transmit only when there are pending frames in its transmission queue. Thus, the transmission probability, τ_v, that the AC_v transmits under unsaturated traffic conditions can be derived by

$$\tau_v = \tau'_v(1-P_{0v}) \tag{7}$$

where P_{0v} is the probability that the transmission queue of the AC_v is empty and will be derived in Section 4.3.

Taking virtual collision into account, an HoB frame transmitted from an AC will collide with HoB frames sent from other stations, or from the higher priority ACs in the same station. Therefore, the collision probability, p_v, of the AC_v is given by

$$p_v = 1 - \prod_{x=0}^{N} (1-\tau_x)^{n-1} \prod_{x>v}^{N} (1-\tau_x) \tag{8}$$

where n denotes the number of stations.

The probability, p_{bv}, that the channel is idle in a time slot after the AIFS period of the AC_v, is the probability that none of the other ACs is transmitting in the given slot

$$p_{bv} = (1 - \tau_v)^{n-1} \prod_{x \neq v} (1 - \tau_x)^n \tag{9}$$

During the AIFS period of the AC_v, the ACs with the priorities lower than or equal to AC_v cannot transmit. As a result, the probability p_{tv}, that the channel is sensed idle in a time slot during the AIFS period of the AC_v after $AIFS_{\min}$, is given by

$$p_{tv} = \prod_{x>v}^{N} (1 - \tau_x)^n \tag{10}$$

4.2. Analysis of the service time

The service time is defined as the time interval from the instant that an HoB frame starts contending for the channel to the instant that the burst is acknowledged following successful transmission or the instant that the HoB frame is discarded due to transmission failures. The service time is composed of two parts: channel access delay and burst transmission delay. The former is the time interval from the instant that the HoB frame reaches to the head of the transmission queue, until it wins the contention and is ready for transmission, or until it is discarded due to transmission failures. The latter is defined as the time duration of transmitting a burst. We denote $E[S_{sv}]$, $E[A_v]$, and $E[B_{sv}]$ as the mean of the service time, channel access delay, and burst transmission delay, respectively, where v represents that the burst is transmitted from an AC_v and s denotes the number of frames successfully transmitted within the burst. Similarly, let $E'[S_v]$, $E'[A_v]$, and $E'[B_v]$ denote the mean of the service time, channel access delay, and burst transmission delay, respectively, when the HoB frame is discarded due to transmission failures. $E[B_{sv}]$ and $E'[B_v]$ can be expressed as

$$\begin{cases} E[B_{sv}] = AIFS_v + s(T_L + T_H + 2T_{SIFS} + T_{ACK}) - T_{SIFS} \\ E'[B_v] = 0 \end{cases} \tag{11}$$

where T_L and T_H denote the transmission time for the frame payload and frame head, respectively. Next, $E[A_v]$ and $E'[A_v]$ are given by

$$\begin{cases} E[A_v] = T_{cv} \sum_{i=0}^{m} \frac{i p_v^i (1-p_v)}{1-p_v^{m+1}} + \bar{\sigma}_v \sum_{i=0}^{m} \sum_{j=0}^{i} \frac{W_{jv}-1}{2} \frac{p_v^i (1-p_v)}{\left(1-p_v^{m+1}\right)} \\ E'[A_v] = T_{cv}(m+1) + \bar{\sigma}_v \sum_{i=0}^{m} \frac{W_{iv}-1}{2} \end{cases} \tag{12}$$

where T_{cv} is the average collision time and $\bar{\sigma}_v$ is the average length of a time slot. p_v^i is the probability that the backoff counter reaches stage i, p_v^{m+1} represents the probability that the HoB frame is discarded due to multiple collisions, $(W_{iv} - 1)/2$ denotes the mean of the backoff counters generated in the ith backoff stage.

Let PT_v denote the probability that at least one of the remaining ACs transmits in a given time slot and PS_x represent the probability that an AC_x successfully transmits, respectively, provided that the AC_v is in the backoff procedure. PT_v and PS_x can be expressed as

$$PT_v = 1 - p_{bv} = 1 - (1 - \tau_v)^{n-1} \prod_{x \neq v} (1 - \tau_x)^n \tag{13}$$

$$PS_x = n\tau_x (1 - \tau_v)^{n-2} \prod_{y \neq v} (1 - \tau_y)^{n-1} \prod_{y>x}^{N} (1 - \tau_y) \tag{14}$$

The average length of a time slot, $\bar{\sigma}_v$, when the AC_v is in the backoff procedure is obtained by considering the fact that the channel is idle with probability $(1 - PT_v)$, a successful transmission from an AC_x occurs with probability PS_x, and a collision happens with probability $(PT_v - \sum_{x=0}^{N} PS_x)$. Thus, $\bar{\sigma}_v$ can be calculated as

$$\bar{\sigma}_v = (1 - PT_v)\sigma + \sum_{x=0}^{N} PS_x T_{sx} + (PT_v - \sum_{x=0}^{N} PS_x) T_{cv} + E[X_v] PT_v \tag{15}$$

where σ is the duration of a physical time slot [16]. T_{sv} denotes the average time of a successful burst transmission from the AC_v and T_{cv} accounts for the average collision time, respectively. $E[X_v]$ represents the total time spent on deferring the AIFS period of the AC_v. Recall that an AC has to go through the AIFS period again if the channel is sensed busy during the deferring procedure, as shown in the sub-Markov chain of Fig. 1, $E[X_v]$ may consist of several attempts for deferring the AIFS period of the AC_v and can be given by

$$E[X_v] = \sum_{u=1}^{\infty} p_{tv}^{d_v} \left(1 - p_{tv}^{d_v}\right)^{u-1} u T_{av} \tag{16}$$

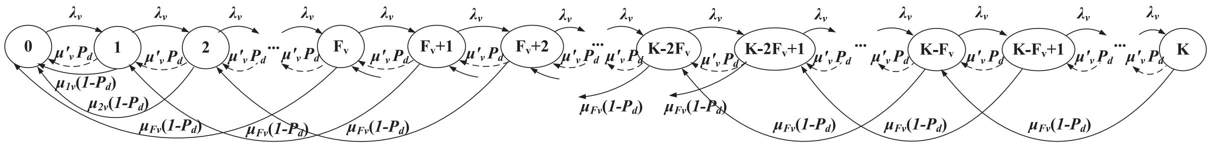

Fig. 2. The state-transition-rate diagram of the $M/G^{[1,F_v]}/1/k$ queueing system.

Table 1
System parameters.

Frame payload	8000 bits	PHY header	192 bits
MAC header	224 bits	ACK	112 bits + PHY header
Date rate	11 Mbit/s	Basic rate	1 Mbit/s
Slot time	20 μs	Buffer size	50 frames
SIFS	10 μs	Retry limit	7

Table 2
EDCA parameters.

Scenarios	ACs	AIFSN	CW_{min}	CW_{max}	TXOP
Scenario 1	AC0	6	32	1024	1 Frame
	AC1	2	32	512	1 Frame
	AC2	2	16	256	4 Frames
	AC3	2	8	128	2 Frames
Scenario 2	AC0	7	64	512	1 Frame
	AC1	4	32	512	1 Frame
	AC2	2	16	256	2 Frames
	AC3	2	16	256	4 Frames

where u is the number of attempts for deferring the AIFS period of the AC_v, T_{av} is the average time spent on each attempt, and $p_{tv}^{d_v}$ is the probability of an successful attempt. T_{av} is given by

$$T_{av} = \sum_{x>v}^{N} PS'_x T_{sx} + (PT' - \sum_{x>v}^{N} PS'_x) T_{cv} + \sum_{s=1}^{d_v-1} p_{tv}^{s} s\sigma \tag{17}$$

where the first and second terms correspond to the "frozen time" of the backoff counter of the AC_v caused by the transmission from the higher priority ACs with the smaller AIFS. The third term is the average time spent on a failed attempt for down-counting the remaining time slots during the AIFS period of the AC_v after $AIFS_{\min}$. PT'_v and PS'_x denote the probabilities that at least one AC transmits and the AC_x successfully transmits in a given time slot, respectively, when the AC_v is deferring in the AIFS period. PT'_v and PS'_x can be written as

$$PT'_v = 1 - p_{tv} = 1 - \prod_{x>v}^{N} (1-\tau_x)^n \tag{18}$$

$$PS'_x = n\tau_x \prod_{y>v}^{N} (1-\tau_y)^{n-1} \prod_{y>\max\{x,v\}}^{N} (1-\tau_y) \tag{19}$$

Note that only the HoB frame is involved in the collision, the collision time, T_{cv}, is given by

$$T_{cv} = T_L + T_H + T_{SIFS} + T_{ACK} + AIFS_v \tag{20}$$

The average time, T_{sv}, for a successful burst transmission from the AC_v can be written as

$$T_{sv} = \frac{\sum_{s=1}^{F_v} E[B_{sv}] L_{sv}}{1 - P_{0v}} \tag{21}$$

where F_v denotes the maximum number of frames that can be transmitted in a TXOP limit of the AC_v, the denominator $(1 - P_{0v})$ means that the occurrence of burst transmission is conditioned on the fact that there is at least one frame in the transmission queue, L_{sv} is the probability that s $(1 \leqslant s \leqslant F_v)$ frames are transmitted from the AC_v within a TXOP limit, and $E[B_{sv}]$ is the burst transmission delay given in Eq. (11).

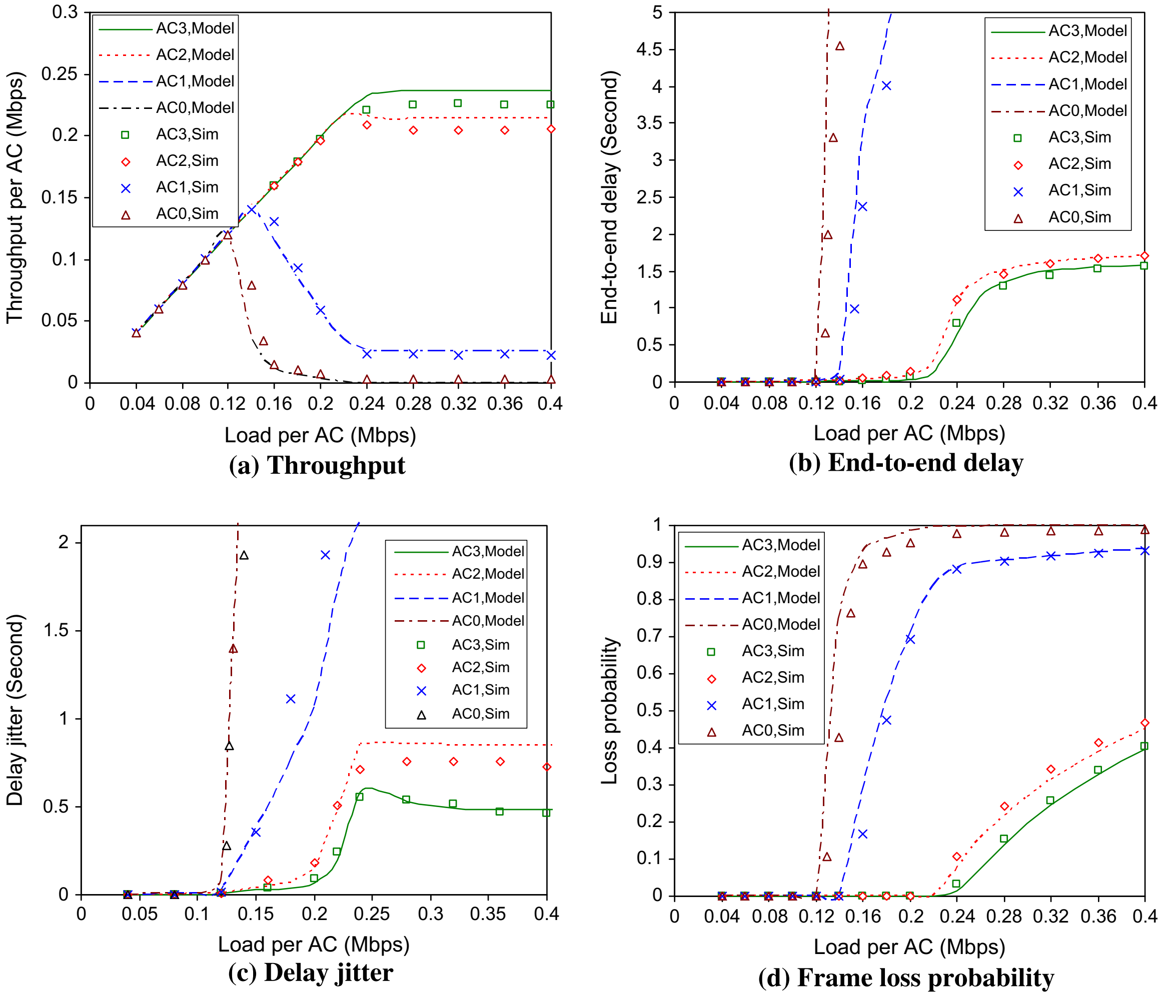

Fig. 3. Performance metrics versus the offered loads per AC in Scenario 1.

4.3. Queueing model

The transmission queue at the AC_v can be modelled as an $M/G^{[1,F_v]}/1/k$ queueing system where the superscript $[1,F_v]$ denotes that the number of frames transmitted during a TXOP ranges from 1 to F_v, and K represents the system capacity.

The server becomes busy when a frame reaches to the head of the transmission queue. The server becomes free after a burst of frames are acknowledged by the destination following successful transmission, or after the HoB frame is dropped due to transmission failures. The service time is dependent on the number of frames transmitted within a burst and the class of the transmitting AC. Thus, the service time of a burst with s $(1 \leqslant s \leqslant F_v)$ frames successfully transmitted from the AC_v can be modelled by an exponential distribution function with mean $E[S_{sv}]$, then the mean service rate, μ_{sv}, is given by $1/E[S_{sv}]$. When the HoB frame is discarded due to transmission failures, the mean service rate, μ'_v, is given by $1/E'[S_v]$.

Fig. 2 illustrates the state-transition-rate diagram of the queueing system of the AC_v where each state denotes the number of frames in the system. The transition rate from state r to $r+1$ $(0 \leqslant r \leqslant K-1)$ is the arrival rate λ_v of the Poisson traffic. A transition from state r to $r-1$ $(1 \leqslant r \leqslant K)$ implies that the HoB frame is dropped due to transmission failures with probability P_d, which is given by p_v^{m+1}, and the transition rate is $\mu'_v P_d$. Then a transition out of state r to $r - F_v$ $(F_v \leqslant r \leqslant K)$ represents that the burst transmission of F_v frames completes and the transition rate is $\mu_{F_v}(1-P_d)$. The change from state r to 0 $(1 \leqslant r \leqslant F_v - 1)$ denotes that all r frames in the queueing system are transmitted within a burst and the transition rate is $\mu_{rv}(1-P_d)$.

We can obtain the transition rate matrix, $\mathbf{G}_v$, of the Markov chain in Fig. 2. The steady-state probability vector, $\mathbf{P}_v = (P_{rv}, r = 0, 1, \ldots, K)$, of the Markov chain satisfies the following equations

$$\mathbf{P}_v \mathbf{G}_v = 0 \quad \text{and } \mathbf{P}_v \mathbf{e} = 1 \tag{22}$$

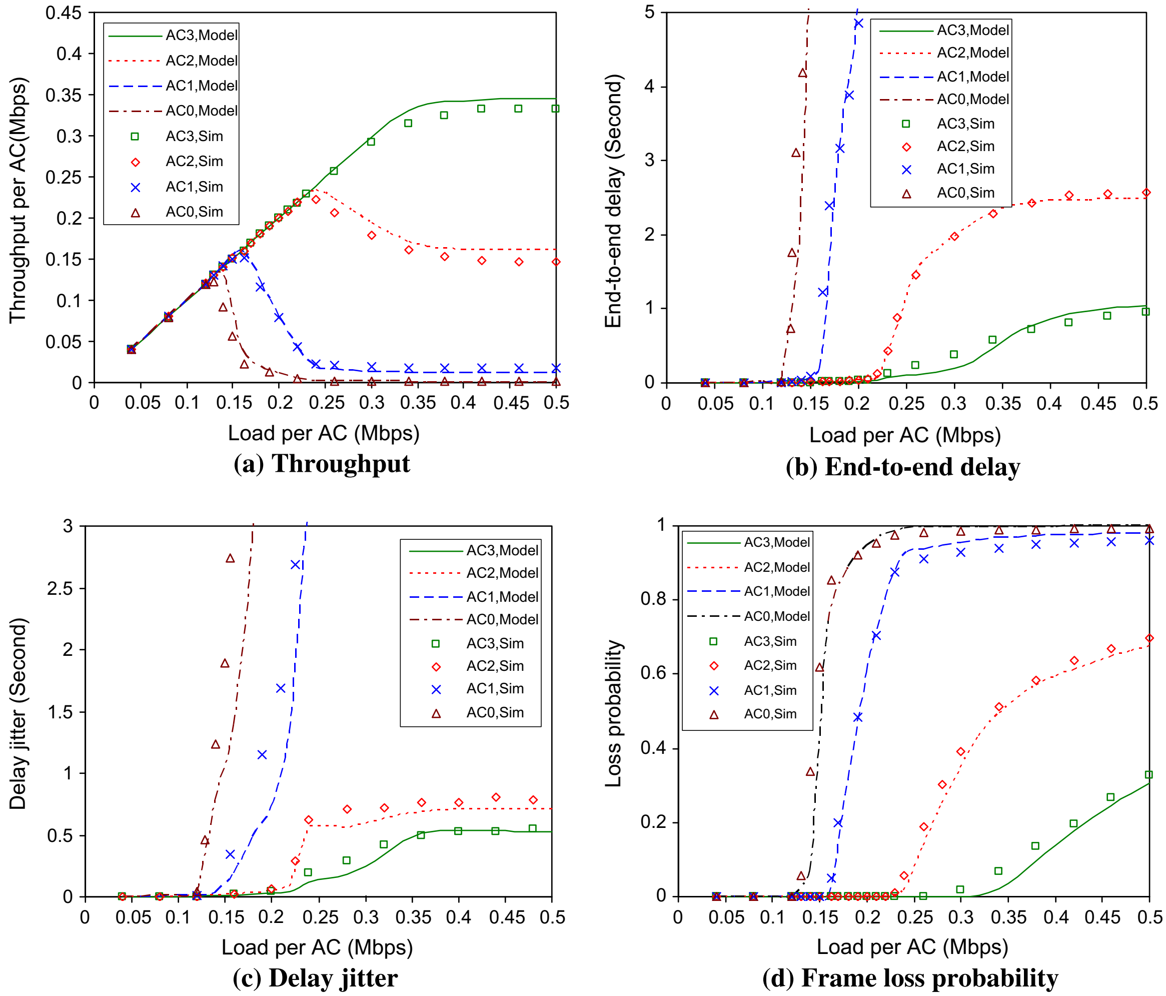

Fig. 4. Performance metrics versus the offered loads per AC in Scenario 2.

where **e** is a unit column vector. After obtaining $\mathbf{P}_v$, we can have the probability that $s(1 \leqslant s \leqslant F_v)$ frames are transmitted from the AC_v within a TXOP limit, L_{sv}, as

$$\begin{cases} L_{sv} = P_{sv}, & 1 \leqslant s < F_v \\ L_{sv} = \sum_{r=F_v}^{K} P_{rv}, & s = F_v \end{cases} \tag{23}$$

The frame loss probability is defined as the probability that an arriving frame finds the finite buffer full, which is given by P_{Kv}. The throughput, TH_v, of the AC_v can be computed by

$$TH_v = \lambda_v E[P](1 - P_{Kv})\left(1 - p_v^{m+1}\right) \tag{24}$$

where $E[P]$ is the frame payload length and p_v^{m+1} is the probability that the frame is dropped due to $(m + 1)$ transmission failures.

The end-to-end delay, which consists of queueing delay and service time, is the time interval from the instant that the frame enters the transmission queue to the instant that the frame is acknowledged after its successful reception. Let T_{Dv} denote the random variable for the end-to-end delay of the frame in AC_v and $P_{Dv}(t)$ denote its Cumulative Distribution Function (CDF). When an arriving frame enters the transmission queue and finds that r frames are in the queueing system, to ensure that the service of this frame completes during time $[0, t]$, all $(r + 1)$ frames including itself must have been served by time t. Therefore, $P_{Dv}(t)$, can be expressed as

$$P_{Dv}(t) = \Pr\{T_{Dv} \leqslant t\} = \sum_{r=0}^{K-1} [\Pr\{r + 1 \text{ completions in } t | \text{arrival finds } r \text{ in the system of } AC_v\} \cdot P'_{rv}] \tag{25}$$

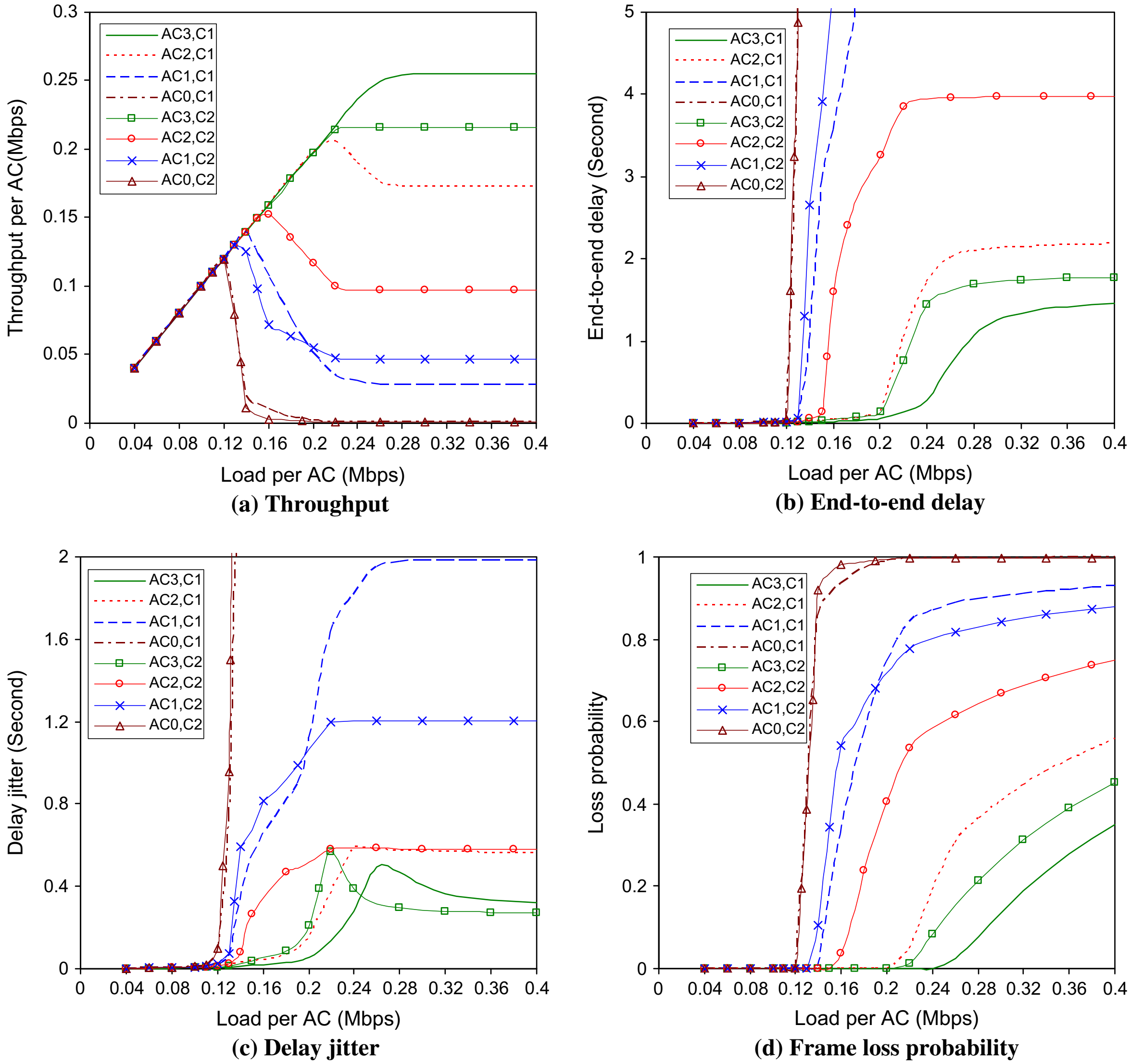

Fig. 5. Performance comparison of EDCA between two distinct cases. Case 1 (C1): EDCA with the AIFS, CW, and TXOP schemes; Case 2 (C2): EDCA with the AIFS and CW schemes.

where P'_{rv} is the probability that an arriving frame enters the transmission queue and finds r frames in the queueing system of AC_v. When the arriving frame finds the queueing system full, it will be dropped from the system. Therefore, P'_{rv}, is given by

$$P'_{rv} = \frac{P_{rv}}{1 - P_{Kv}}, \quad r \leqslant K - 1 \tag{26}$$

where P_{rv} is the probability that there are r frames in the queueing system of AC_v upon the arrival of the new frame. P_{rv} is identical to the steady state distribution of system size since the input process is Poisson.

Since the dropped frames due to multiple collisions are excluded in the calculation of the end-to-end delay and the transmission queue of AC_v is modelled as a bulk service queueing system, $(r + 1)$ frames are served in $r'(r' = \lceil (r + 1)/F_v \rceil)$ bursts where each of $\lfloor (r + 1)/F_v \rfloor$ bursts has F_v frames and the last burst has $[(r + 1) - \lfloor (r + 1)/F_v \rfloor \cdot F_v]$ frames. Due to the memoryless nature of the service time of individual bursts, the distribution of the service time required for r' bursts is independent of the arrival time of the frame and is the convolution of r' exponential random variables, which is a hypo-exponential distribution [4]. Specifically, if let $X_{iv}(1 \leqslant i \leqslant r')$ represent independent exponential random variables with respective rates $\mu^i_v(1 \leqslant i \leqslant r')$, random variable $\sum_{i=1}^{r'} X_{iv}$ follows a hypo-exponential distribution. Based on Eq. (25), $P_{Dv}(t)$, can be written as

$$P_{Dv}(t) = \sum_{r=0}^{K-1} P'_{rv} \int_0^t f_{rv}(x)dx \tag{27}$$

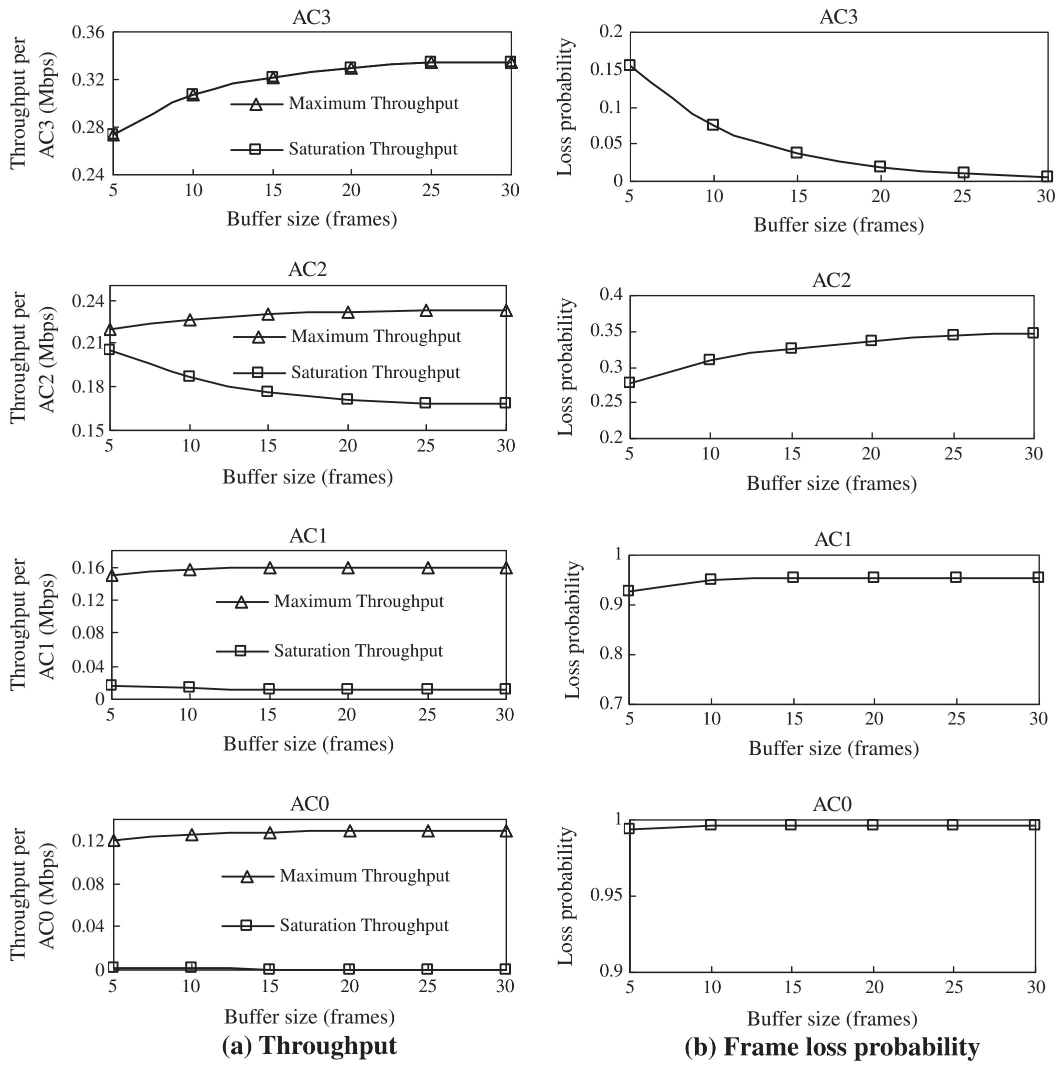

Fig. 6. Analytical performance results against the buffer size: (a) throughput; (b) loss probability; (c) end-to-end delay; and (d) delay jitter.

where $f_{rv}(x)$ is the probability density function (pdf) of the hypo-exponential distribution with r' ($r' = \lceil (r+1)/F_v \rceil$) states. As a special case of the phase-type distribution [4], the hypo-exponential distribution can be written in the form of a phase-type distribution with the representation $(\mathbf{S}, \boldsymbol{\alpha})$ where $\mathbf{S}$ is a $r' \times r'$ matrix with diagonal elements $-\mu_v^i$ $(1 \leqslant i \leqslant r')$ and super-diagonal elements μ_v^i and $\boldsymbol{\alpha}$ denotes the probability that the service process starts in each of the r' state. $\mathbf{S}$ and $\boldsymbol{\alpha}$ are given by

$$\mathbf{S} = \begin{bmatrix} -\mu_v^i & \mu_v^i & & & & \\ & -\mu_v^i & \mu_v^i & & & \\ & & \ddots & \ddots & & \\ & & & -\mu_v^i & \mu_v^i & \\ & & & & -\mu_v^i & \mu_v^i \\ & & & & & -\mu_v^i \end{bmatrix}, \quad \boldsymbol{\alpha} = (1, 0, \ldots, 0) \tag{28}$$

μ_v^i is given by

$$\mu_v^i = \begin{cases} \mu_{Fv}, 1 \leqslant i < r' \quad \text{and } r' > 1 \\ \mu_{sv}, i = r', s = [(r+1) - \lfloor (r+1)/F_v \rfloor \cdot F_v] \end{cases} \tag{29}$$

where $\mu_{sv}(1 \leqslant s \leqslant F_v)$ is the service rate of the burst with s frames transmitted from AC_v.

Then the pdf, $f_{rv}(x)$, of the hypo-exponential distribution can be expressed as [4]

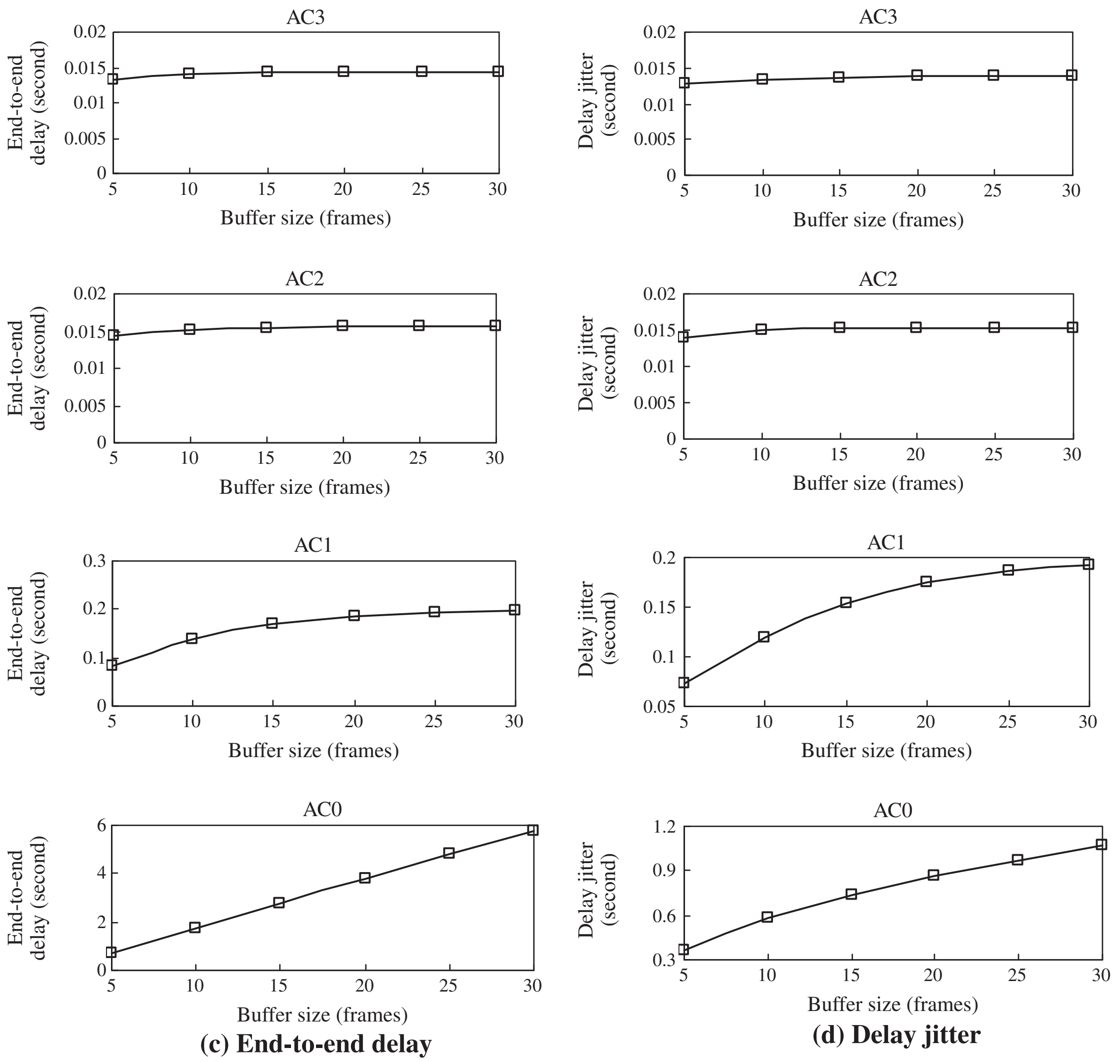

Fig. 6 (*continued*)

$$f_{rv}(x) = -\boldsymbol{\alpha}\exp(x\mathbf{S})\mathbf{Se} \tag{30}$$

where **e** is a unit column vector of the size r' and exp (**S**) denotes the matrix exponential of **S**.

With the CDF of the end-to-end delay, $P_{Dv}(t)$, its mean (delay) and standard deviation (delay jitter) can be given by

$$E[D_v] = \int_0^\infty t dP_{Dv}(t) \tag{31}$$

$$\sigma[D_v] = \sqrt{\int_0^\infty t^2 dP_{Dv}(t) - E[D_v]^2} \tag{32}$$

5. Model validation and performance evaluation

In this section, we first investigate the accuracy of the proposed analytical model through extensive NS-2 simulation experiments and then use the model to evaluate the performance of three QoS differentiation schemes in EDCA.

5.1. Model validation

To validate the accuracy of this model, we compare the analytical performance results against those obtained from the NS-2 simulation experiments of the IEEE 802.11e EDCA [39]. We consider a WLAN with 10 stations located in a

100 m × 100 m rectangular grid. Each station has four ACs, which are denoted by subscripts 0, 1, 2, and 3 from the lowest to highest priority. The packet arrivals at each AC are characterized by a Poisson process. The system parameters used in this study are summarized in Table 1.

To investigate the accuracy of the model under various working conditions, we consider two scenarios with the different combinations of EDCA parameters, as shown in Table 2. Figs. 3 and 4 depict the results of throughput, end-to-end delay, delay jitter, and frame loss probability versus the offered loads per AC in Scenarios 1 and 2, respectively. The close match between the analytical results and those obtained from simulation experiments demonstrates that the proposed model can produce the accurate performance results of EDCA with AIFS, CW and TXOP under arbitrary traffic loads. Moreover, as shown in Fig. 3, it is worth mentioning that the maximum throughputs of AC_1 and AC_0 are much larger than their saturation throughput (the same phenomenon can be found in Fig. 4 with AC_2, AC_1, and AC_0). This observation emphasizes the importance of analyzing the EDCA protocol under unsaturated traffic loads.

5.2. Performance evaluation

In this subsection, the proposed analytical model is used to investigate the effects of the TXOP scheme and the buffer size on the QoS performance of the IEEE 802.11e EDCA protocol.

5.2.1. Effects of the TXOP scheme

The existing studies on performance analysis of EDCA have been mainly focused on the AIFS, CW, and TXOP schemes, separately. However, the proposed analytical model enables to conduct a comprehensive evaluation of the QoS differentiation schemes in EDCA integrating the three schemes. Fig. 5 plots the curves of the throughput, end-to-end delay, delay jitter, and frame loss probability versus the offered loads per AC with different settings of TXOP limits. For thepurpose of comparison, two distinct cases are considered: (1) the TXOP limits of AC_3, AC_2, AC_1, and AC_0 in Case 1 are set to 2, 3, 1, and 1 (frame), respectively; (2) the TXOP limits of all ACs in Case 2 are identical and equal to 1 (frame), which means that the TXOP scheme is not enabled. All the other EDCA parameters are the same as those used in Scenario 1, as shown in Table 2. For clarity of performance analysis, the offered loads per AC (from 0 to 0.4 Mbps) is divided into three regions where 0–0.12 Mbps is the light load region, 0.12–0.22 Mbps is the medium load region, and 0.22–0.4 Mbps is the heavy load region.

Under the light load region, the TXOP scheme has little impact on the performance of the ACs as the throughput, end-to-end delay, delay jitter, and frame loss probability of the ACs are almost the same in both cases. However, it can be observed that the TXOP scheme has a significant impact on the performance of the ACs under the medium and heavy load regions. Specifically, compared with Case 2, the throughput, end-to-end delay, and frame loss probability of AC_3 and AC_2 ameliorate largely while those of AC_1 and AC_0 deteriorate in Case 1 when the ACs are under the heavy load region. However, different from the other performance metrics, the delay jitter of AC_3 increases while that of $AC_2$is almost the same in Case 1 compared to those in Case 2. The reason is that bulk service can increase the delay jitter of a frame when the finite buffer queueing system is under heavy loads. It is interesting to note that the QoS of all the ACs in Case 1 is better than those in Case 2 under the medium load region. The QoS of AC_3 and AC_2 is improved due to the burst transmission in these ACs. However, the impact of burst transmission of AC_3 and AC_2 over the performance of AC_1 and AC_0 depends on the traffic load region. Under the medium load region, burst transmission of AC_3 and AC_2 may make their transmission queues empty frequently and thus reduces the number of contending ACs, which leads to the lower collision probabilities for AC_1 and AC_0. However, under the heavy load region, the burst transmission of AC_3 and AC_2 cannot reduce the number of contending ACs since the transmission queues of AC_3 and AC_2 are always backlogged. Moreover, the burst transmission of AC_3 and AC_2 enables them to obtain long channel occupation time. As a result, the performance of AC_1 and $AC_0$is degraded. The above observations demonstrate that the TXOP scheme cannot only provide service differentiation like AIFS and CW, but also improve the system performance.

5.2.2. Effects of the buffer size

Most existing models for EDCA under unsaturated traffic conditions assumed that the MAC buffer has either a very small size [20,34] or an infinite capacity [1,6,7,25,36], because the assumption of a small buffer could avoid considering queuing dynamics while the infinite buffer assumption could reduce the difficulty of developing the queuing model. However, these unrealistic assumptions, as to be shown later, can cause considerable inaccuracies of analytical results. Using the proposed model, we reveal the impact of the buffer size on the QoS performance of EDCA in terms of throughput, end-to-end delay, delay jitter, and frame loss probability. Fig. 6 depicts the performance of each AC as a function of the buffer size with the EDCA parameters of Scenario 2, as shown in Table 2. We plot the maximum throughput and saturation throughput of each AC with different buffer sizes in Fig. 6a. In Fig. 6b, the loss probability performance is presented with the traffic loads per AC of 0.3 Mbps. The end-to-end delay and delay jitter are also depicted in Fig. 6c and d respectively, when the traffic loads per AC are at 0.16 Mbps. It is clear that the throughput (both the maximum and saturation throughput) and loss probability of AC_3 and AC_2 vary largely when the buffer size increases from 5 to 20 and then change little as the buffer size further augments. In contrast, for the AC_1 and AC_0, the throughput and loss probability are hardly affected by the buffer size. On the other hand, the end-to-end delay and delay jitter of AC1 and AC0 soar as the buffer size increases while those of AC3 and AC2 only slightly change with the buffer size. These results clearly demonstrate that the MAC buffer size has a significant impact on the QoS performance of ACs in the IEEE 802.11e WLANs.

6. Conclusions

This paper has presented a comprehensive analytical model to accommodate the QoS differentiation schemes in terms of AIFS, CW, and TXOP specified in the IEEE 802.11e EDCA protocol with finite buffer capacity and unsaturated traffic loads. This model employs an approach combining the Markov chain and queueing theory to analyze the backoff procedure and the burst transmission procedure in EDCA. The QoS performance measures including throughput, end-to-end delay, delay jitter, and frame loss probability have been derived and further validated through extensive NS-2 simulation experiments. The analytical model has been used for performance analysis of EDCA. Numerical results have shown that, the TXOP scheme can support service differentiation between various ACs and also improve the network performance, whereas the AIFS and the CW schemes can provide QoS differentiation only. The model has also been used to investigate the effects of the MAC buffer size on the QoS performance of EDCA. The results have revealed that the buffer size has considerable impact on the QoS performance of EDCA. The comprehensiveness, efficiency, and accuracy of the proposed analytical model make it a cost-effective tool for the performance evaluation of the IEEE 802.11e WLANs. Possible future work involves extending the analytical model and simulation validation to account for more practical physical layer models, such as bursty channel errors and link adaptation with modulation and coding scheme (MCS). We also plan to validate the analytical model against experimental measurements in a real testbed to further improve the impact of the model.

References

[1] O. Abu-Sharkh, A. Tewfik, Toward accurate modeling of the IEEE 802.11e EDCA under finite load and error-prone channel, IEEE Transactions on Wireless Communications 7 (7) (2008) 2560–2570.
[2] A. Banchs, P. Serrano, L. Vollero, Providing service guarantees in 802.11e EDCA WLANs with legacy stations, IEEE Transactions on Mobile Computing 9 (8) (2010) 1057–1071.
[3] G. Bianchi, Performance analysis of the IEEE 802.11 distributed coordination function, IEEE Journal on Selected Areas in Communications 18 (3) (2000) 535–547.
[4] L. Breuer, D. Baum, An Introduction to Queueing Theory and Matrix-Analytic Methods, Springer, 2005.
[5] L. Cai, X. Shen, J.W. Mark, L. Cai, Y. Xiao, Voice capacity analysis of WLAN with unbalanced traffic, IEEE Transactions on Vehicular Technology 55 (3) (2006) 752–761.
[6] X. Chen, H. Zhai, X. Tian, Y. Fang, Supporting QoS in IEEE 802.11e wireless LANs, IEEE Transactions on Wireless Communications 5 (8) (2006) 2217–2227.
[7] P.E. Engelstad, O.N. Osterbo, Analysis of the total delay of IEEE 802.11e EDCA and 802.11 DCF, Proceedings of the IEEE ICC'06 2 (2006) 552–559.
[8] D. Gao, J. Cai, C.H. Foh, C.T. Lau, K.N. Ngan, Improving WLAN VoIP capacity through service differentiation, IEEE Transactions on Vehicular Technology 57 (1) (2008) 65–474.
[9] K. Ghaboosi, M. Latva-aho, Y. Xiao, B.H. Khalaj, Modeling nonsaturated contention-based IEEE 802.11 multihop ad hoc networks, IEEE Transactions on Vehicular Technology 58 (7) (2009) 3518–3532.
[10] J. Hu, G. Min, M.E. Woodward, Analysis and comparison of burst transmission schemes in unsaturated 802.11e WLANs, Proceedings of the IEEE GLOBECOM'07 (2007) 5133–5137.
[11] J. Hu, G. Min, M.E. Woodward, W. Jia, A comprehensive analytical model for IEEE 802.11e QoS differentiation schemes under unsaturated traffic loads, Proceedings of the IEEE ICC'08 (2008) 241–245.
[12] C.L. Huang, W. Liao, Throughput and delay performance of IEEE 802.11e enhanced distributed channel access (EDCA) under saturation condition, IEEE Transactions on Wireless Communications 6 (1) (2007) 136–145.
[13] J. Hui, M. Devetsikiotis, A unified model for the performance analysis of IEEE 802.11e EDCA, IEEE Transactions on Communications 53 (9) (2005) 1498–1510.
[14] B.J. Hwang, I.S. Hwang, W.R. Chen, Adaptive radio resource management for interactive user-centric IPTV services in mobile WiMAX networks, Elsevier Information Sciences 181 (18) (2011) 4024–4040.
[15] H.Y. Hwang, S.J. Kim, D.K. Sung, N.O. Song, Performance analysis of IEEE 802.11e EDCA with a virtual collision handler, IEEE Transactions on Vehicular Technology 57 (2) (2008) 1293–1297.
[16] IEEE, Wireless LAN Medium Access Control (MAC) and Physical Layer (PHY) specifications: Medium Access Control (MAC) Quality of Service (QoS) Enhancements, IEEE Standard 802.11e, 2005.
[17] I. Inan, F. Keceli, E. Ayanoglu, Analysis of the 802.11e enhanced distributed channel access function, IEEE Transactions on Communications 57 (6) (2009) 1753–1764.
[18] A. Khan, D. Smith, S. Hussein, H. Helgert, Performance analysis of VoIP Codecs over multi-rate EDCA, Proceedings of the IEEE CCNC'12 (2012) 110–115.
[19] A.M. Khedr, W. Osamy, Minimum perimeter coverage of query regions in a heterogeneous wireless sensor network, Elsevier Information Sciences 181 (15) (2011) 3130–3142.
[20] S. Kim, R. Huang, Y. Fang, Deterministic priority channel access scheme for QoS support in IEEE 802.11e wireless LANs, IEEE Transactions on Vehicular Technology 58 (2) (2009) 855–864.
[21] Z. Kong, D. Tsang, B. Bensaou, D. Gao, Performance analysis of IEEE 802.11e contention-based channel access, IEEE Journal on Selected Areas in Communications 22 (10) (2004) 2095–2106.
[22] M. Laddomada, F. Mesiti, M. Mondin, F. Daneshgaran, On the throughput performance of multirate IEEE 802.11 networks with variable-loaded stations: analysis, modeling, and a novel proportional fairness criterion, IEEE Transactions on Wireless Communications 9 (5) (2010) 1594–1607.
[23] T. Li, Q. Ni, Y. Xiao, Investigation of the block ACK scheme in wireless ad-hoc networks, Wireless Communications and Mobile Computing 6 (6) (2006) 877–888.
[24] L. Lin, H. Fu, W. Jia, An efficient admission control for IEEE 802.11 networks based on throughput analysis of (un)saturated channel, Proceedings of the IEEE GLOBECOM'05 5 (2005) 3017–3021.
[25] J. Liu, Z. Niu, Delay analysis of IEEE 802.11e EDCA under unsaturated conditions, Proceedings of the IEEE WCNC'07 (2007) 430–434.
[26] G. Min, J. Hu, M.E. Woodward, An analytical model of the TXOP scheme with heterogeneous classes of stations, Proceedings of the IEEE GLOBECOM'08 (2008).
[27] A. Nafaa, A. Ksentini, On sustained QoS guarantees in operated IEEE 802.11 wireless LANs, IEEE Transactions on Parallel and Distributed Systems 19 (8) (2008) 1020–1033.
[28] S.H. Nguyen, H.L. Vu, L.L.H. Andrew, Performance analysis of IEEE 802.11 WLANs with saturated and unsaturated sources, IEEE Transactions on Vehicular Technology 61 (1) (2012) 333–345.
[29] F. Peng, B. Peng, D. Qian, Performance analysis of IEEE 802.11e enhanced distributed channel access, IET Communications 4 (6) (2010) 728–738.
[30] V. Ramaiyan, A. Kumar, E. Altman, Fixed point analysis of single cell IEEE 802.11e WLANs: uniqueness and multistability, IEEE/ACM Transactions on Networking 16 (5) (2008) 1080–1093.

[31] J.W. Robinson, T.S. Randhawa, Saturation throughput analysis of IEEE 802.11e enhanced distributed coordination function, IEEE Journal on Selected Areas in Communications 22 (5) (2004) 917–928.
[32] M. Saleem, G. Di Caro, M. Farooq, Swarm intelligence based routing protocol for wireless sensor networks: survey and future directions, Elsevier Information Sciences 181 (20) (2011) 4597–4624.
[33] J.W. Tantra, C.H. Foh, A.B. Mnaouer, Throughput and delay analysis of the IEEE 802.11e EDCA saturation, Proceedings of the IEEE ICC'05 5 (2005) 3450–3454.
[34] J.W. Tantra, C.H. Foh, I. Tinnirello, G. Bianchi, Analysis of the IEEE 802.11e EDCA under statistical traffic, Proceedings of the IEEE ICC'06 2 (2006) 546–551.
[35] Z. Tao, S. Panwar, Throughput and delay analysis for the IEEE 802.11e enhanced distributed channel access, IEEE Transactions on Communications 54 (4) (2006) 596–603.
[36] O. Tickoo, B. Sikdar, Modeling queueing and channel access delay in unsaturated IEEE 802.11 random access MAC based wireless networks, IEEE/ACM Transactions on Networking 16 (4) (2008) 878–891.
[37] I. Tinnirello, S. Choi, Efficiency analysis of burst transmission with block ACK in contention-based 802.11e WLANs, Proceedings of the IEEE ICC'05 5 (2005) 3455–3460.
[38] S. Tursunova, Y.T. Kim, Realistic IEEE 802.11e EDCA model for QoS-aware mobile cloud service provisioning, IEEE Transactions on Consumer Electronics 58 (1) (2012) 60–68.
[39] S. Wietholter, M. Emmelmann, C. Hoene, A. Wolisz, TKN EDCA Model for ns-2, Technical Report TKN-06-003, Technical University of Berlin, 2006.
[40] Y. Xiao, Performance analysis of priority schemes for IEEE 802.11 and IEEE 802.11e wireless LANs, IEEE Transactions on Wireless Communications 4 (4) (2005) 1506–1515.
[41] D. Xu, T. Sakurai, H.L. Vu, An access delay model for IEEE 802.11e EDCA, IEEE Transactions on Mobile Computing 8 (2) (2009) 261–275.
[42] H. Zhu, I. Chlamtac, Performance analysis for IEEE 802.11e EDCF service differentiation, IEEE Transactions on Communications 4 (4) (2005) 1779–1788.